Stoichiometric and Catalytic Reactions Involving Si−H Bond Activations by Rh and Ir Complexes Containing a Pyridylindolide Ligand

Dmitry Karshtedt,[†,‡] Alexis T. Bell,*[,§,‡] and T. Don Tilley*[,†,‡]

Departments of Chemistry and Chemical Engineering, University of California, Berkeley, Berkeley, California 94720, and Chemical Sciences Division, Lawrence Berkeley National Laboratory, 1 Cyclotron Road, Berkeley, California 94720

Received June 5, 2006

New rhodium and iridium complexes containing the bidentate, monoanionic 2-(2′-pyridyl)indolide (PyInd) ligand were prepared. The bis(ethylene) complex (PyInd)Rh(C_2H_4)$_2$ (**3**) reacted with triethylsilane at 60 °C to produce the 16-electron Rh(V) bis(silyl)dihydride complex (PyInd)RhH_2($SiEt_3$)$_2$ (**4**). Both **3** and **4** catalyzed the chloride transfer reaction of chlorobenzene and Et_3SiH to give Et_3SiCl and benzene in the absence of base. In the presence of LiN^iPr_2, catalytic C−Si coupling was observed, to produce Et_3SiPh. Analogous Ir complexes of the type (PyInd)IrH_2(SiR_3)$_2$, where R_3 = Et_3 (**6a**), Me_2Ph (**6b**), Ph_2Me (**6c**), or Ph_3 (**6d**), were not catalytically active in this chloride transfer chemistry. The molecular structure of **6c**, determined by X-ray crystallography, may be described as having a highly unusual bicapped tetrahedral geometry. DFT calculations indicate that this distortion is associated with the d^4 electron count and the presence of highly *trans*-influencing silyl ligands. The reaction of **6a** with PMe_3 (5 equiv) produced (PyInd)IrH($SiEt_3$)(PMe_3)$_2$ (**7**), while the reaction with PPh_3 (1 equiv) generated a mixture of isomers that was converted to (PyInd)IrH($SiEt_3$)(PPh_3) (**8**) upon heating in benzene at 80 °C. Complexes **7** and **8** exhibit regular octahedral and distorted square pyramidal geometries, respectively.

Introduction

Activation of Si−H bonds by oxidative addition to late transition metal complexes is a fundamental step in a number of catalytic transformations involving organosilanes.[1] These include an industrially important Pt-based system for the hydrosilation of olefins,[2] as well as potentially valuable processes such as dehydrogenative silane polymerization,[3] silane redistribution,[4] and silane reduction of haloarenes.[5] The oxidative addition of a Si−H bond to a metal center has also been implicated as a key step in Rh- and Pt-catalyzed arylsilane syntheses via the dehydrogenative coupling of silanes and arenes[6] and in related systems involving silanes and haloarenes.[7] Such Si−C coupling reactions are of considerable interest, since arylsilanes have recently begun to replace their boron- and tin-containing analogues as substrates for Pd-catalyzed cross-coupling chemistry.[8] Arylsilanes have a number of advantages over these traditionally employed reagents, since they are generally more tolerant of functional groups than boronic acids and less toxic than stannanes.

Complexes of Rh and Ir exhibit particularly rich Si−H bond activation chemistry due to the ability of these metals to support mononuclear silyl complexes in a variety of oxidation states.[9−14] In addition, these metals are known to form η^2-silane complexes, which can be described as products of incomplete oxidative addition of a Si−H bond.[15] Thus, silane activations by Rh and Ir continue to attract attention because they offer a variety of

* To whom correspondence should be addressed. E-mail: tdtilley@berkeley.edu.

† Department of Chemistry, University of California, Berkeley.

§ Department of Chemical Engineering, University of California, Berkeley.

‡ Lawrence Berkeley National Laboratory.

(1) (a) Tilley, T. D. In *The Chemistry of Organic Silicon Compounds*; Patai, S., Rappoport, Z., Eds.; Wiley: New York, 1989; Chapter 24, p 1415. (b) Ojima, I. In *The Chemistry of Organic Silicon Compounds*; Patai, S., Rappoport, Z., Eds.; Wiley: New York, 1989; Chapter 24, p 1479. (c) Tilley, T. D. *Comments Inorg. Chem.* **1990**, *10*, 37. (d) Tilley, T. D. In *The Silicon-Heteroatom Bond*; Patai, S., Rappoport, Z., Eds.; Wiley: New York, 1991; Chapters 9 and 10, pp 245−309. (e) Corey, J. Y.; Braddock-Wilking, J. *Chem. Rev.* **1999**, *99*, 175.

(2) Marciniec, B., Gulinski, J., Urbaniak, W., Kornetka, Z. W., Eds. *Comprehensive Handbook on Hydrosilation*; Pergamon: Oxford, 1992.

(3) (a) Brook, M. A. *Silicon in Organic, Organometallic, and Polymer Chemistry*; Wiley: New York, 2000. (b) Aitken, C. T.; Harrod, J. F.; Samuel, E. *J. Am. Chem. Soc.* **1986**, *108*, 4059. (c) Tilley, T. D. *Acc. Chem. Res.* **1993**, *26*, 22. (d) See also: Fontaine, F.-G.; Zargarian, D. *J. Am. Chem. Soc.* **2004**, *126*, 8786, and references therein.

(4) (a) Hashimoto, H.; Tobita, H.; Ogino, H. *J. Organomet. Chem.* **1995**, *499*, 205. (b) Radu, N. S.; Hollander, F. J.; Tilley, T. D.; Rheingold, A. L. *Chem. Commun.* **1996**, *21*, 2459. (c) Gavenonis, J.; Tilley, T. D. *Organometallics* **2004**, *23*, 31.

(5) (a) Alonso, F.; Beletskaya, I. P.; Yus, M. *Chem. Rev.* **2002**, *102*, 4009. (b) Boukherroub, R.; Chatgiliaoglu, C.; Manuel, G. *Organometallics* **1996**, *15*, 1508. (c) Esteruelas, M. A.; Herrero, J.; López, F. M.; Martín, M.; Oro, L. A. *Organometallics* **1999**, *18*, 1110. (d) Díaz, J.; Esteruelas, M. A.; Herrero, J.; Moralejo, L.; Oliván, M. *J. Catal.* **2000**, *195*, 187.

(6) (a) Ezbiansky, K.; Djurovich, P. I.; LaForest, M.; Sinning, D.; Zayes, R.; Berry, D. H. *Organometallics* **1998**, *17*, 1455. (b) Tsukada, N.; Hartwig, J. F. *J. Am. Chem. Soc.* **2005**, *127*, 5022.

(7) (a) Murata, M.; Suzuki, K.; Watanabe, S.; Masuda, Y. *J. Org. Chem.* **1997**, *62*, 8569. (b) Manoso, A. S.; DeShong, P. *J. Org. Chem.* **2001**, *66*, 7449. (c) Murata, M.; Ishikura, M.; Nagata, M.; Watanabe, S.; Masuda, Y. *Org. Lett.* **2002**, *4*, 1843.

(8) (a) Denmark, S. E.; Sweis, R. F. In *Metal-Catalyzed Cross-Coupling Reactions*; de Mejere, A., Diedrich, F., Eds.; Wiley-VCH: Weinheim, Germany, 2004; pp 163−216. (b) Denmark, S. E.; Ober, M. H. *Aldrichim. Acta* **2003**, *36*, 75. (c) Horn, K. A. *Chem. Rev.* **1995**, *95*, 1317. (d) Hatanaka, Y.; Hiyama, T. *Synlett* **1991**, 845.

(9) Examples of Rh(I)−silyl complexes: (a) Goikhman, R.; Milstein, D. *Chem.--Eur. J.* **2005**, *11*, 2983. (b) Goikhman, R.; Aizenberg, M.; Ben-David, Y.; Shimon, L. J. W.; Milstein, D. *Organometallics* **2002**, *21*, 5060. (c) Okazaki, M.; Ohshitanai, S.; Tobita, H.; Ogino, H. *J. Chem. Soc., Dalton Trans.* **2002**, 2061. (d) Aizenberg, M.; Ott, J.; Elsevier, C. J.; Milstein, D. *J. Organomet. Chem.* **1998**, *551*, 81. (e) Hofmann, P.; Meier, C.; Hiller, W.; Heckel, M.; Riede, J.; Schmidt, M. U. *J. Organomet. Chem.* **1995**, *490*, 51. (f) Thorn, D. L.; Harlow, R. L. *Inorg. Chem.* **1990**, *29*, 2017. (g) Joslin, F. L.; Stobart, S. R. *J. Chem. Soc., Chem. Commun.* **1989**, 504.

10.1021/om060492+ CCC: $33.50
Publication on Web 08/09/2006

strategies for the design of catalytic cycles. While a number of group 9 complexes containing cyclopentadienyl-[6a,10a,b,11,13b,14e] and phosphine-based[9,10d−h,12,13d−n,14a−c] ligands have been shown to promote Si−H bond activation, analogous systems with nitrogen donor ligands remain relatively unexplored.[13c,14d] The presence of hard nitrogen donor ligands on soft transition metals such as Rh or Ir is expected to enable the (NN)Rh and (NN)Ir fragments to support high oxidation state complexes.[16]

Recently, bidentate ligands that feature localized neutral and anionic nitrogen donors have begun to attract interest because of their ability to support reactive late transition metal species. For example, platinum complexes of 2-(2′-pyridyl)indolide (PyInd)[17] and the related 2-(*N*-arylimino)pyrrolide[18] ligands have been observed to mediate catalytic and stoichiometric transformations of arenes, respectively. While the chemistry of group 9 metals containing such ligands has so far remained unexplored, their successful application in Pt-promoted hydrocarbon activations suggests that Rh and Ir complexes of NN* (NN* = PyInd or a related ligand) should be reactive toward bond activations via oxidative addition. Along these lines, the concomitant activation of silanes and chlorobenzene, generally considered to be a relatively inert substrate due to the strength of the aromatic C−Cl bond, represents a particularly interesting goal.[19] A possible outcome of a catalyzed reaction between PhCl and a silane is chloride transfer from carbon to silicon, resulting in production of benzene and a silyl chloride. In fact, such a transformation has been realized with triethylsilane, using Pd or Rh catalysts.[5b−d] A different reaction pathway, however, can lead to formation of a C−Si bond, accompanied by the elimination of HCl. Such a reaction has not been achieved with PhCl, although analogous Rh-catalyzed processes that utilize PhBr or PhI in combination with triethoxysilane and stoichiometric base have been reported.[7] It was envisioned that reactive (PyInd)M (M = Rh, Ir) fragments might provide a platform for examining successive activations of silanes and PhCl and enable the development of catalytic reactions involving these substrates.

This report describes activations of silanes by PyInd complexes of Rh and Ir. The (PyInd)Rh fragment catalyzes both the established chloride transfer process that generates Et_3SiCl from PhCl and Et_3SiH and the novel base-promoted Ph−Si coupling between these substrates. These reactions involve an unusual, isolable 16-electron Rh(V) bis(triethylsilyl)dihydride species. In contrast, the (PyInd)Ir fragment does not participate in this catalysis, but provides access to a range of stable Ir(V) bis(silyl)dihydrides. Structural studies and DFT calculations demonstrate that these d^4 complexes feature a rare, highly distorted bicapped tetrahedral geometry. This work underscores the utility of reactive, high-valent intermediates in the development of catalytic silane conversions.

Results and Discussion

Synthesis of (PyInd)Rh Complexes. Previous studies demonstrated that the potassium salt K[PyInd] is a convenient transfer agent for the 2-(2′-pyridyl)indolide ligand.[17a] Thus, K[PyInd] was used to prepare several Rh(I) complexes via salt metathesis with chloride-bridged precursors of the type $[L_2RhCl]_2$. For example, K[PyInd] reacted with $[(CO)_2RhCl]_2$ at room temperature in benzene to give (PyInd)Rh(CO)$_2$ (**1**) in 76% yield (eq 1) after extraction with CH_2Cl_2 and crystallization from a CH_2Cl_2/pentane mixture. The IR spectrum of **1** contains two carbonyl stretching frequencies at 2054 and 1999 cm^{-1}, which may reflect slightly greater π-back-bonding in this neutral complex relative to the cationic analogue $[(bpy)Rh(CO)_2]^+$ (ν_{CO} at 2080 and 2010 cm^{-1}).[20]

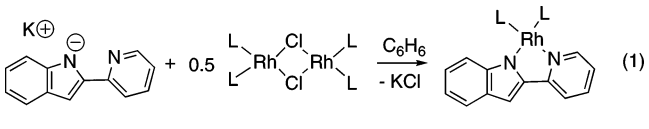

1: L = CO
2: L_2 = COD
3: L = C_2H_4

(10) Rh(III): (a) Ampt, K. A. M.; Duckett, S. B.; Perutz, R. N. *Dalton Trans.* **2004**, 3331. (b) Taw, F. L.; Mueller, A. H.; Bergman, R. G.; Brookhart, M. *J. Am. Chem. Soc.* **2003**, *125*, 9808. (c) Tse, A. K.-S.; Wu, B.-M.; Mak, T. C. W.; Chan, K. S. *J. Organomet. Chem.* **1998**, *568*, 257. (d) Nishihara, Y.; Takemura, M.; Osakada, K. *Organometallics* **2002**, *21*, 825. (e) Mitchell, G. P.; Tilley, T. D. *Organometallics* **1998**, *17*, 2912. (f) Auburn, M. J.; Stobart, S. R. *Inorg. Chem.* **1985**, *24*, 318. (g) Ebsworth, E. A. V.; De Ojeda, M. R.; Rankin, D. W. H. *J. Chem. Soc., Dalton Trans.* **1982**, 1513. (h) Haszeldine, R. N.; Parish, R. V.; Taylor, R. J. *J. Chem. Soc., Dalton. Trans.* **1974**, 2311. (i) See also: Osakada, K. *J. Organomet. Chem.* **2000**, *611*, 323, and references therein.

(11) Rh(V): (a) Cook, K. S.; Incarvito, C. D.; Webster, C. E.; Fan, Y. B.; Hall, M. B.; Hartwig, J. F. *Angew. Chem., Int. Ed.* **2004**, *43*, 5474. (b) Duckett, S. B.; Perutz, R. N. *J. Chem. Soc., Chem. Commun.* **1991**, 28. (c) Duckett, S. B.; Haddleton, D. M.; Jackson, S. A.; Perutz, R. N.; Poliakoff, M.; Upmacis, R. K. *Organometallics* **1988**, *7*, 1526. (d) Fernandez, M.-J.; Maitlis, P. M. *J. Chem. Soc., Dalton Trans.* **1984**, 2063. (e) Fernandez, M.-J.; Bailey, P. M.; Bentz, P. O.; Ricci, J. S.; Koetzle, T. F.; Maitlis, P. M. *J. Am. Chem. Soc.* **1984**, *106*, 5458.

(12) Examples of Ir(I)−silyl complexes: (a) Okazaki, M.; Tobita, H.; Ogino, H. *Chem. Lett.* **1998**, 69. (b) Aizenberg, M.; Milstein, D. *Organometallics* **1996**, *15*, 3317. (c) Okazaki, M.; Tobita, H.; Ogino, H. *Organometallics* **1996**, *15*, 2790.

(13) Ir(III): (a) Simons, R. S.; Panzner, M. J.; Tessier, C. A.; Youngs, W. J. *J. Organomet. Chem.* **2003**, *681*, 1. (b) Klei, S. R.; Tilley, T. D.; Bergman, R. J. *Organometallics* **2002**, *21*, 3376. (c) Stradiotto, M.; Fujdala, K. L.; Tilley, T. D. *Chem. Commun.* **2001**, 1200. (d) Brost, R. D.; Bruce, G. C.; Joslin, F. L.; Stobart, S. R. *Organometallics* **1997**, *16*, 5669. (e) Okazaki, M.; Tobita, H.; Ogino, H. *Chem. Lett.* **1997**, 437. (f) Esteruelas, M. A.; Olivan, M.; Oro, L. A. *Organometallics* **1996**, *15*, 814. (g) Aizenberg, M.; Milstein, D. *J. Am. Chem. Soc.* **1995**, *117*, 6456. (h) Cleary, B. P.; Mehta, R.; Eisenberg, R. *Organometallics* **1995**, *14*, 2297. (i) Burger, P.; Bergman, R. G. *J. Am. Chem. Soc.* **1993**, *115*, 10462. (j) Rappoli, B. J.; McFarland, J. M.; Thompson, J. S.; Atwood, J. D. *J. Coord. Chem.* **1990**, *21*, 147. (k) Auburn, M. J.; Holmes-Smith, R. D.; Stobart, S. R. *J. Am. Chem. Soc.* **1984**, *106*, 1314. (l) Ebsworth, E. A. V.; Fraser, T. E.; Henderson, S. G.; Leitch, D. M.; Rankin, D. W. H. *J. Chem. Soc., Dalton Trans.* **1981**, 1010. (m) Glockling, F.; Irwin, J. G. *Inorg. Chim. Acta* **1972**, *6*, 355. (n) Harrod, J. F.; Gilson, D. F. R.; Charles, R. *Can. J. Chem.* **1969**, *47*, 2205.

(14) Ir(V): (a) Turculet, L.; Feldman, J. D.; Tilley, T. D. *Organometallics* **2004**, *23*, 2488. (b) Feldman, J. D.; Peters, J. C.; Tilley, T. D. *Organometallics* **2002**, *21*, 4065. (c) Loza, M.; Faller, J. W.; Crabtree, R. H. *Inorg. Chem.* **1995**, *34*, 2937. (d) Gutierrez-Puebla, E.; Monge, A.; Paneque, M.; Poveda, M. L.; Taboada, S.; Trujillo, M.; Carmona, E. *J. Am. Chem. Soc.* **1999**, *121*, 346. (e) Klei, S. R.; Tilley, T. D.; Bergman, R. G. *J. Am. Chem. Soc.* **2000**, *122*, 1816. (f) Tanke, R. S.; Crabtree, R. H. *Organometallics* **1991**, *10*, 415. (g) Fernandez, M.-J.; Maitlis, P. M. *Organometallics* **1983**, *2*, 164.

(15) (a) Schubert, U. *Adv. Organomet. Chem.* **1990**, *30*, 151. (b) Bart, S. C.; Lobkovsky, E.; Chirik, P. J. *J. Am. Chem. Soc.* **2004**, *126*, 13794. (c) Taw, F. L.; Bergman, R. G.; Brookhart, M. *Organometallics* **2004**, *23*, 886. (d) Lin, Z. *Chem. Soc. Rev.* **2002**, *31*, 239. (e) Delpech, F.; Sabo-Etienne, S.; Chaudret, B.; Daran, J.-C. *J. Am. Chem. Soc.* **1997**, *119*, 3167. (f) Schneider, J. J. *Angew. Chem., Int. Ed. Engl.* **1996**, *35*, 1069.

(16) For examples of high oxidation state late transition metal complexes supported by nitrogen-based ligands, see: (a) Rendina, L. M.; Puddephatt, R. J. *Chem. Rev.* **1997**, *97*, 1735. (b) van Asselt, R.; Rijnberg, E.; Elsevier, C. J. *Organometallics* **1994**, *13*, 706. (c) Canty, A. J. *Acc. Chem. Res.* **1992**, *25*, 83.

(17) (a) Karshtedt, D.; Bell, A. T.; Tilley, T. D. *Organometallics* **2004**, *23*, 4169. (b) Karshtedt, D.; McBee, J. L.; Bell, A. T.; Tilley, T. D. *Organometallics* **2006**, *25*, 1801.

(18) Iverson, C. N.; Carter, C. A. G.; Baker, R. T.; Scollard, J. D.; Labinger, J. A.; Bercaw, J. E. *J. Am. Chem. Soc.* **2003**, *125*, 12674.

(19) (a) Grushin, V. V.; Alper, H. *Top. Organomet. Chem.* **1999**, *3*, 193. (b) Grushin, V. V.; Alper, H. *Chem. Rev.* **1994**, *94*, 1047.

(20) Reddy, G. K. N.; Ramesh, B. R. *J. Organomet. Chem.* **1974**, *67*, 443.

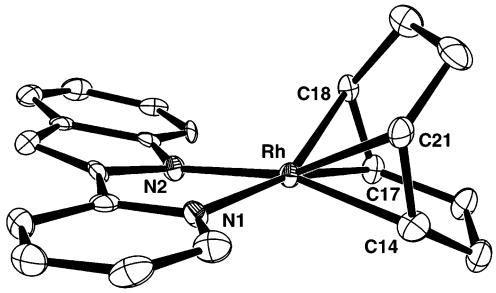

Figure 1. ORTEP diagram of the molecular structure of (PyInd)Rh(COD) (**2**), showing one of the two crystallographically independent molecules of **2** present in the asymmetric unit (with the ligand fragments canted at the angle of 11°). Hydrogen atoms were omitted for clarity. Selected bond lengths (Å): Rh−N1 = 2.111(5), Rh−N2 = 2.058(5), Rh−C14 = 2.107(6), Rh−C21 = 2.120(7), Rh−C17 = 2.118(6), Rh−C18 = 2.141(6), C14−C21 = 1.389(8), C17−C18 = 1.393(8). Bond angle (deg): N1−Rh−N2 = 79.7(2).

The diolefin complex (PyInd)Rh(COD) (**2**) was also prepared in high yield (93%) via a salt methathesis route, starting from K[PyInd] and $[(COD)RhCl]_2$ (eq 1). The solid-state structure of **2** was determined by X-ray crystallography and is shown in Figure 1. As expected, the PyInd ligand is nearly planar and the olefinic fragments of the cyclooctadiene ligands are perpendicular to the (NN*)Rh plane. The N−Rh−N angle is approximately 80°, indicating that PyInd enforces a smaller bite angle than that typically observed in Rh complexes of the related β-diiminate ligands (approximately 90°), which feature a six-membered chelate ring.[21] Interestingly, two crystallographically independent molecules of the complex are present in the asymmetric unit of the primitive monoclinic space group $P2_1/n$. The primary difference between the two molecules is a rotation of the pyridinyl group with respect to the indolyl group (dihedral angle of 1° in one rotamer and of 11° in the other rotamer). This result suggests that the energy barrier to a slight canting of the PyInd ligand is quite low.

Complex **2** was found to be quite inert toward triethylsilane, as no changes were observed in the ^{1}H NMR spectrum when a mixture of **2** and excess Et_3SiH (5 equiv) was heated in benzene-d_6 at 130 °C for 12 h. Since this lack of reactivity may be ascribed to the presence of the chelating, nonlabile cyclooctadiene ligand, a more reactive Rh(I) precursor was sought. This was accomplished using $[(C_2H_4)_2RhCl]_2$, which reacted cleanly with K[PyInd] (eq 1) to yield the (bis)ethylene complex (PyInd)Rh$(C_2H_4)_2$ (**3**). The ^{1}H NMR spectrum of **3** contains four distinct, slightly broadened vinylic resonances (1.98, 2.39, 2.75, and 4.82 ppm). The upfield shift of these resonances relative to that of free ethylene (5.24 ppm) points to a significant degree of back-bonding from the Rh(I) center to the carbon−carbon double bond.[22] Presumably, as in complex **2**, the olefin ligands are perpendicular to the (NN*)Rh plane, resulting in chemically inequivalent environments for the four pairs of vinylic hydrogens. The ethylene orientation is further confirmed by the ^{13}C{^{1}H} NMR spectrum of **3**, which contains only two resonances for these ligands at 60.8 (J_{RhC} = 12.5 Hz) and 63.2 ppm (br).

Activation of 4 equiv of Et_3SiH by **3** resulted in formation of the bis(silyl)dihydride complex (PyInd)$RhH_2(SiEt_3)_2$ (**4**) upon heating in benzene at 60 °C over the course of 2 h (eq 2). In addition, 2 equiv of tetraethylsilane byproduct formed as a result of ethylene ligand hydrosilation. Complex **4** is not crystalline, but it can be isolated in 71% yield as an analytically pure oily red solid upon lyophilization of the crude product from benzene, followed by a cold pentane wash to remove $SiEt_4$. The ^{1}H NMR spectrum of **4** features two hydride resonances at −15.32 ppm (J_{RhH} = 28.5 Hz) and −13.88 ppm (J_{RhH} = 23.5 Hz), while its ^{29}Si{^{1}H} NMR spectrum exhibits only one resonance at 63.0 ppm (J_{RhSi} = 26.8 Hz). The value of the H−H coupling constant, 9.0 Hz, is typical for an unsymmetrical rhodium *cis*-dihydride species.[23] In addition, the Si−H coupling constants associated with the two hydrides, which were observed in the ^{29}Si dimension of the *J*-resolved ^{1}H−^{29}Si gradient heteronuclear multiple bond correlation (gHMBC) spectrum,[24] were found to be 8.1 and 6.2 Hz, respectively. Generally, silyl hydride complexes with J_{SiH} values below 20 Hz are considered to have no η^2-silane ligand character.[1e] Thus, the J_{SiH} values suggest that complex **4** can be viewed as a Rh(V) bis(silyl)dihydride. Moreover, the unexceptional rhodium−hydride T_1 values[25,26] (1.1 and 1.2 s, determined at 500 MHz and 25 °C using the null method) are quite consistent with a classical dihydride structure, while the bands characteristic of Rh−H bonds (2065, 2090 cm^{-1}) in the IR spectrum also support the presence of pentavalent rhodium in **4**.[9c,11d,e,23a] The J_{SiH}, T_1, and IR data obtained for **4** are similar to those reported for the analogous 18-electron complex $Cp^*RhH_2(SiEt_3)_2$, for which the oxidation state of 5 for the Rh center was confirmed by determination of the hydride positions by neutron diffraction.[11e]

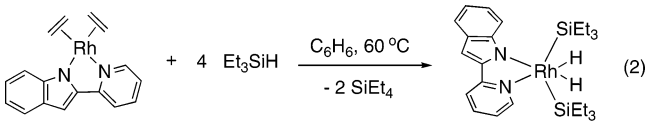

3 **4** (2)

Complex **4** catalyzed the complete isomerization of 5 equiv of 1-octene to a mixture of internal octenes (70 °C, 4 h, benzene-d_6), a result that is also consistent with the presence of a hydride ligand in **4**. However, Si−H bond elimination from **4** is facile, as addition of excess PMe_3 to **4** in benzene-d_6 at room temperature resulted in formation of 2 equiv of Et_3SiH and a species formulated as (PyInd)Rh$(PMe_3)_2$ by ^{1}H and ^{31}P{^{1}H} NMR spectroscopy (see Experimental Section). Unfortunately, this complex could not be isolated, as removal of the solvent under reduced pressure led to its decomposition. Furthermore, attempts to synthesize (PyInd)$RhH_2(SiR_3)_2$ species from silanes other than Et_3SiH did not meet with success. For example, a reaction of **3** with triphenylsilane appeared to result in a dihydride species analogous to **4** (as judged by ^{1}H NMR spectroscopy), but this complex could not be obtained in pure form.

Catalyzed Reactions of Silanes with PhCl. The observed chemistry of **3** prompted the examination of this complex as a catalyst for reactions involving Si−H and Ph−Cl bond activations. Consistent with expectations, **3** catalyzed the reaction of 10 equiv of Et_3SiH with neat PhCl at 80 °C over the course of

(21) Willems, S. T. H.; Budzelaar, P. H. M.; Moonen, N. N. P.; de Gelder, R.; Smits, J. M. M.; Gal, A. W. *Chem.--Eur. J.* **2002**, *8*, 1310.

(22) (a) Maire, P.; Breher, F.; Schönberg, H.; Grützmacher, H. *Organometallics* **2005**, *24*, 3207. (b) Hahn, C. *Chem.--Eur. J.* **2004**, *10*, 5888.

(23) (a) Ezhova, M. B.; Patrick, B. O.; Sereviratne, K. N.; James, B. R.; Waller, F. J.; Ford, M. E. *Inorg. Chem.* **2005**, *44*, 1482. (b) Heinrich, H.; Giernoth, R.; Bargon, J.; Brown, J. M. *Chem. Commun.* **2001**, 1296.

(24) Meissner, A.; Sorensen, O. W. *Magn. Reson. Chem.* **2001**, *39*, 49.

(25) (a) Hamilton, D. G.; Crabtree, R. H. *J. Am. Chem. Soc.* **1988**, *110*, 4126. (b) Ammann, C.; Isaia, F.; Pregosin, P. S. *Magn. Reson. Chem.* **1988**, *26*, 236. (c) Desrosiers, P. J.; Cai, L.; Lin, Z.; Richards, R.; Halpern, J. *J. Am. Chem. Soc.* **1991**, *113*, 4173.

(26) This method of determining the presence of H−H interactions has been shown to be somewhat unreliable for a family of osmium polyhydride complexes; see Desrosiers et al.[25c]

Scheme 1. Proposed Mechanism for the Silylation of Chlorobenzene

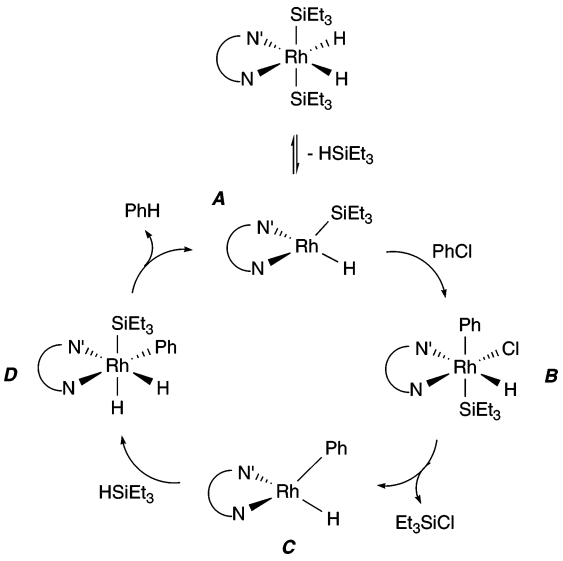

20 h to produce Et_3SiCl in 77% yield (eq 3). Complex **4** was the only Rh-containing species observed in solution during the course of catalysis (by ^1H NMR spectroscopy), as it formed readily under these conditions and persisted until the reaction was complete. In addition, 2 equiv of $SiEt_4$ were detected by GC-MS (using tetraphenylsilane as the internal standard), confirming that the ethylene ligands were removed via hydrosilation. Isolated complex **4** also catalyzed chloride transfer from PhCl to yield Et_3SiCl, at a rate similar to that obtained with **3** (10 equiv of Et_3SiH were consumed at 80 °C in 16 h). This result demonstrates that **4** is a kinetically competent intermediate in this transformation.

$$Et_3SiH + PhCl \xrightarrow[80\ ^\circ C,\ 20\ h]{10\ mol\ \%\ \mathbf{3}} Et_3SiCl + PhH \qquad (3)$$

The catalytic action of **3** on arylsilanes, under the reaction conditions similar to those employed with Et_3SiH (neat PhCl, 80 °C, 20 h), was dominated by redistribution chemistry at silicon.[27] For example, **3** catalyzed the conversion of Ph_2MeSiH to a mixture of Ph_3SiMe, Ph_2SiH_2, and other silicon-containing products. The silane Ph_3SiMe was observed when the catalytic reaction was conducted in chorobenzene or cyclohexane, demonstrating that PhCl was not required to deliver the additional phenyl group to silicon. Similar results were obtained with Me_2PhSiH, which reacted to give Me_2SiPh_2, Me_2SiH_2, and other silicon-containing products, while Ph_3SiH was unreactive in this system. In contrast, **3** catalyzed the chlorination of 10 equiv of $^tBu_2SiH_2$ in chlorobenzene (80 °C, 40 h) to yield a mixture of $^tBu_2HSiCl$ (67%) and $^tBu_2SiCl_2$ (9%), and no products of redistribution of the alkyl groups at silicon were detected. For all of the substrates other than Et_3SiH, complicated mixtures containing several Rh hydride species were observed by ^1H NMR spectroscopy during the course of catalysis.

Although the mechanism of chloride transfer from PhCl to Et_3SiH is not yet fully understood, we believe that it involves reductive elimination of Et_3SiH from **4** to give a reactive 14-electron Rh(III) intermediate **A** (Scheme 1). This species may activate PhCl to provide the key hydrido-chloride Rh(V) intermediate **B**. Subsequent reductive elimination of Et_3SiCl from **B** appears to be reasonable because it leads to the formation of a strong Si−Cl bond. This step may be followed by the oxidative addition of Et_3SiH and loss of benzene, regenerating intermediate **A**. While the initiation of a catalytic cycle by reductive elimination from a 16-electron species may appear to be unusual, precedent for such a step can be found in the Ir-pincer alkane dehydrogenation system, where the 14-electron (PCP)Ir fragment (derived via loss of H_2 from $(PCP)IrH_2$) is thought to be the catalytically active species.[28] An alternative mechanism for chloride transfer catalysis by (PyInd)Rh may involve a modified associative mechanism. In this pathway, one of the silyl hydride fragments is converted to an η^2-silane ligand, allowing for oxidative addition of PhCl to form an 18-electron intermediate. While the formation of such a crowded seven-coordinate species appears to be less favorable compared to that of a 14-electron mono(silyl)hydride, neither mechanism can be ruled out on the basis of the available data. The possibility that some of the steps in the catalytic cylcle involve σ-bond metathesis processes, rather than discrete oxidative additions and reductive eliminations, must also be considered.

To reverse the selectivity of the coupling process to obtain Et_3SiPh rather than Et_3SiCl (eq 4), it is necessary to consume the HCl byproduct that would be generated. If intermediate **B** is involved, this can be achieved by a base-promoted reductive elimination of HCl from the Rh(V) center.[29] This type of a transformation has in fact been realized with a Rh catalyst, using bromobenzene and triethoxysilane in the presence of a stoichiometric amount of a tertiary amine.[7c] With $(EtO)_3SiH$ as a potential coupling substrate, however, silane redistribution was the dominant pathway. Thus, when **3** and 10 equiv of $(EtO)_3SiH$, along with 10 equiv of triethylamine, were heated in PhCl for 16 h at 90 °C, $Si(OEt)_4$ was found to be the major product (approximately 80% yield), and only traces (<5%) of $(EtO)_3SiPh$ were detected by GC-MS. As a result, Et_3SiH, which exhibits no tendency to undergo redistribution, was utilized in further attempts to develop Rh-catalyzed dehydrochlorinative couplings of PhCl with silanes.

$$Et_3SiH + PhCl + base \xrightarrow[90\ ^\circ C,\ 20\ h]{10\ mol\ \%\ \mathbf{3}} Et_3SiPh + base(HCl) \qquad (4)$$

Initial studies centered on use of alkylamine bases to direct the catalytic transformation toward C−Si bond formation. This approach proved promising, as observable amounts of Et_3SiPh (ca. 5% by GC-MS) were formed in the presence of stoichiometric triethylamine or diisopropylethylamine (conditions as in eq 4). It was reasoned, however, that these bases did not remove HCl efficiently enough to reverse the selectivity of silyl group transfer. Thus, efforts to improve reaction yields focused on the utilization of additives that would effect chloride abstraction or substitution in addition to deprotonation. This was thought to be necessary because formation of the Si−Cl bond provides a strong thermodynamic driving force toward the chlorosilane coupling product. To this end, a number of Lewis/Bronsted base combinations were screened (Table 1). Although both $AlCl_3$/$^iPr_2NEt$ and $AlCl_3$/DBU shifted reaction selectivity from Et_3SiCl to Et_3SiPh, only 3 or 4 turnovers could be achieved. This result may be attributed to the reactive nature of the $AlCl_3$ additive,

(27) Redistribution of arylsilanes is frequently observed as an undesired side reaction in other Rh-catalyzed silane transformations, but the mechanism of this process is poorly understood. See, for example: Rosenberg, L.; Davis, C. W.; Yao, J. *J. Am. Chem. Soc.* **2001**, *123*, 5120, and references therein. Researchers should be cautioned that this process may generate pyrophoric silane gas as a byproduct.

(28) Renkema, K. B.; Kissin, Y. V.; Goldman, A. S. *J. Am. Chem. Soc.* **2003**, *125*, 7770.

(29) Grushin, V. V. *Acc. Chem. Res.* **1993**, *26*, 279.

Table 1. Effects of Additives on the Catalytic Dehydrochlorinative Silylation of PhCl[a]

entry	additive[b]	yield of Et_3SiPh (%)	yield of Et_3SiCl[c] (%)
1	$^iPr_2NEt$	7	84
2	NEt_3	5	87
3	$AlCl_3/NEt_3$	14	15
4	$AlCl_3/^iPr_2NEt$	39	5
5	$AlCl_3$/DBU	31	8
6	$GaCl_3/^iPr_2NEt$	0	0
7	$AgOTf/^iPr_2NEt$	0	0
8	$NBu_4I/^iPr_2NEt$	9	77
9	KHMDS	35	52
10	LiHMDS	42	48
11	LDA	70	5

[a] Conditions as in eq 4. [b] 1.2 equiv relative to Et_3SiH. [c] Observed as Et_3SiOH or $Et_3SiOSiEt_3$ by GC, except for entries 9−11, where Et_3SiCl was converted to the corresponding silylamine in situ.

which appeared to cause rapid decomposition of the Rh catalyst.[30]

Alkali metal bases proved to be particularly effective for the sequestration of chloride (Table 1). Potassium hexamethyldisilazide (KHMDS), lithium hexamethyldisilazide (LiHMDS), and lithium diisopropylamide (LDA) were examined, with LDA providing the highest selectivity for C−Si coupling (70% yield of Et_3SiPh).[31] A relatively small amount of *N*,*N*-diisopropylaniline (23%), the product of the reaction between chlorobenzene and excess lithium amide, was also detected by GC-MS. Nonetheless, this amine could be easily separated from the Et_3SiPh product on a silica column.

Although this catalysis requires a strong amide base, the unusual coupling of PhCl with an alkylsilane demonstrates that the thermodynamically favored Si−Cl bond-forming pathway can be overcome with the aid of appropriate additives. The requirement for a stoichiometric amount of LDA limits potential applications of this system to substrates that contain no acidic or highly electrophilic functionalities. Nevertheless, it is noteworthy that the same Rh complex **3** catalyzes both arene dechlorination and dehydrochlorinative silylation, depending on the reaction conditions.[32]

Synthesis and Characterization of Ir(V) Bis(silyl)dihydrides. The interesting catalytic and stoichiometric reactivity of **3** with Et_3SiH prompted an investigation of similar species containing iridium. Initially, these efforts were hampered by the lack of appropriate Ir(I) precursors. Similar to its Rh analogue **2**, the complex (PyInd)Ir(COD) (**5**), prepared from K[PyInd] and $[(COD)IrCl]_2$, was unreactive toward Et_3SiH. Thus, preparation of a (bis)monoolefin Ir(I) complex from K[PyInd] and $[(COE)_2IrCl]_2$ was attempted. This was unsuccessful, as the transiently formed (NN*)Ir(I) species appeared to activate the cyclooctene ligands to give a mixture of Ir hydrides. It was found, however, that the direct combination of K[PyInd], $[(COE)_2IrCl]_2$, and 4 equiv of Et_3SiH resulted in clean formation of the bis(triethylsilyl)dihydride $(PyInd)IrH_2(SiEt_3)_2$ (**6a**) at room temperature (67% yield). The ^1H NMR spectrum of **6a** features two inequivalent hydrides at −18.04 and −15.53 ppm that exhibit small H−H coupling (^2J = 2.0 Hz). Both the ^{29}Si chemical shift (37.1 ppm) and the magnitudes of the Si−H coupling constants for **6a** were determined using a *J*-resolved $^1H-^{29}Si$ gHMBC experiment (vide supra). The J_{SiH} values obtained for the hydrides in **6a**, 6.4 and 6.7 Hz, are close to those determined for the rhodium analogue **4**, and similarly suggest the lack of η^2-silane character in this complex.

Table 2. Key NMR Data for Ir(V) Complexes 6a−6d[a]

	^1H (ppm)	^{29}Si (ppm)	J_{SiH} (Hz)	T_1 (s)[b]
6a	−15.53	37.1	6.7	1.1
	−18.04		6.4	1.2
6b	−14.84	9.6	12.1	1.2
	−17.36		9.5	1.3
6c	−13.87	7.2	14.2	1.2
	−16.59		11.7	1.3
6d	−13.05	9.2	17.4	1.0
	−16.06		12.5	1.1

[a] All spectra were obtained in benzene-d_6. [b] Obtained at 500 MHz and 25 °C using the null method.

Details of the reaction that generates **6a** are not known, but the lack of an observable cyclooctene hydrosilation product suggests that COE ligands dissociate from the Ir center before silane oxidative addition. This behavior is different from that noted in the preparation of **4**, in which the olefin ligands are removed by hydrosilation with excess Et_3SiH. The absence of the requirement for COE hydrosilation suggests that 2 equiv of the silane are sufficient to prepare **6a**, and this is indeed borne out experimentally (eq 5).

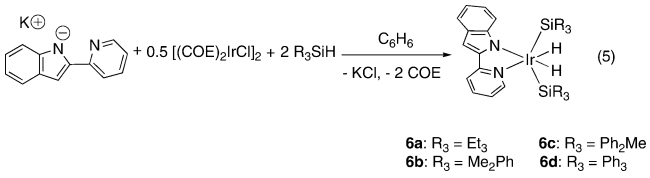

In contrast to its Rh analogue **4**, **6a** did not catalyze chloride transfer from chlorobenzene to triethylsilane or promote dehydrochlorinative C−Si coupling between these substrates in the presence of base (LDA). Indeed, **6a** remained unchanged upon heating in chlorobenzene in the presence of 10 equiv of Et_3SiH and 12 equiv of LDA for 40 h at 150 °C, as the amide became converted to *N*,*N*-diisopropylaniline through a direct aromatic substitution. This lack of reactivity may be attributed to the fact that **6a** is more resistant than its Rh(V) analogue to reductive elimination of Et_3SiH. Moreover, **6a** generally exhibits much greater thermal stability than **4**. While **4** underwent complete decomposition to unidentified species upon heating in benzene-d_6 at 90 °C over the course of 10 h, complex **6** required thermolysis at 190 °C for 20 h (benzene-d_6, sealed tube) before any detectable signs of decomposition were observed by ^1H NMR spectroscopy.

Although **6a** was not an active catalyst for chloride transfer from PhCl, complexes **6a**−**d** were examined as potential structural models for **4**, an isolated intermediate in Rh-catalyzed C−Si coupling of PhCl and Et_3SiH for which an X-ray crystal structure could not be obtained. To this end, bis(arylsilyl) complexes **6b**, **6c**, and **6d** were prepared in high yields, as shown above in eq 5, using 2 equiv of Me_2PhSiH, Ph_2MeSiH, and Ph_3SiH, respectively, in one-pot reactions with K[PyInd] and $[(COE)_2IrCl]_2$. Key NMR data for complexes **6a**−**6d** are summarized in Table 2. Although the values of the Si−H coupling constants for the hydrides in these complexes increase with an increasing number of phenyl groups on Si, all are smaller than 20 Hz, indicating that the Si−H bonds have undergone complete oxidative addition to the Ir center.[1e]

(30) Direct Friedel−Crafts reactions between arenes and chlorosilanes mediated by $AlCl_3$ have been observed, but they typically give arylsilane products in very low yields: Olah, G. A.; Bach, T.; Surya Prakash, G. K. *J. Org. Chem.* **1989**, *54*, 3770.

(31) Resonances in the ^1H NMR spectra acquired when this reaction was monitored were significantly broadened.

(32) Recently, a Pd-based catalytic system was reported for which both iodoarene silylation and reduction with tertiary silanes were observed, depending on reaction conditions: Yamanoi, Y. *J. Org. Chem.* **2005**, *70*, 9607.

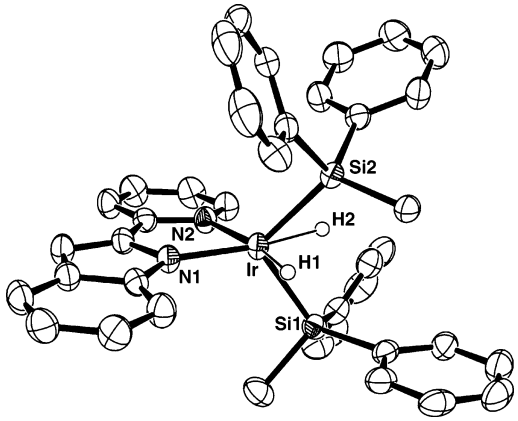

Figure 2. ORTEP diagram of the molecular structure of (PyInd)-$IrH_2(SiPh_2Me)_2$ (**6c**). Hydrogen atoms, except for the iridium hydrides, were omitted for clarity. Selected bond lengths (Å): Ir−Si1 = 2.326(1), Ir−Si2 = 2.338(1), Ir−N1 = 2.016(3), Ir−N2 = 2.149(3), Ir−H1 = 1.61(2), Ir−H2 = 1.60(2). Selected bond angles (deg): Si1−Ir−Si2 = 105.71(3), N1−Ir−N2 = 78.0(1), Si1−Ir−H1 = 81(1), Si1−Ir−H2 = 63(1), Si2−Ir−H1 = 67(1), Si2−Ir−H2 = 55(1).

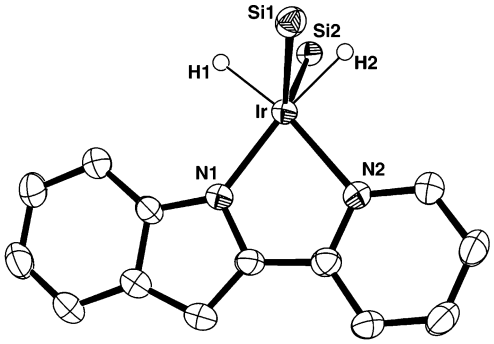

Figure 3. Top view of the X-ray crystal structure of **6c** (hydrogen atoms and substituents on the silicon atoms were omitted for clarity).

Moreover, the T_1 values for all of the hydrides are unexceptional, suggesting the lack of dihydrogen ligand character in these complexes (Table 2).[25,26] Thus, on the basis of these NMR characterizations, complexes **6a**−**6d** can be viewed as Ir(V) species with a d^4 electron count.

The solid-state structure of the diphenylmethylsilane derivative **6c** was determined by X-ray crystallography and is shown in Figure 2. The hydride ligands were located in the Fourier difference map. The Ir−H distances (Ir−H1 = 1.60(2) Å, Ir−H2 = 1.61(2) Å) are similar to typical bond lengths for iridium hydrides determined by neutron diffraction (1.58−1.59 Å).[33] The molecular structure of **6c** features a highly unusual bicapped tetrahedral geometry, with the tetrahedron defined by the silicon and nitrogen atoms. Alternatively, this can be viewed as an extremely distorted octahedral geometry, with the Si−Ir−Si bond angle involving the "*trans*" silyl ligands severely compressed to 105.7°. It is also notable that the Si−Ir−Si plane does not bisect the N−Ir−N angle, as expected in a typical tetrahedral structure, but "leans" toward the pyridinyl side of the PyInd ligand (Figure 3). This leaning does not seem to result from an interaction between the silyl and hydride ligands, since the Si−H distances are too long (closest Si−H contact: 1.93 Å) to invoke η^2-silane complex character in **6c**.[1e,15d,34] In addition, the silicon centers are nearly tetrahedral, a fact that also argues against the presence of an η^2-silane ligand.[35] Thus, the origin of this secondary distortion is not fully apparent.

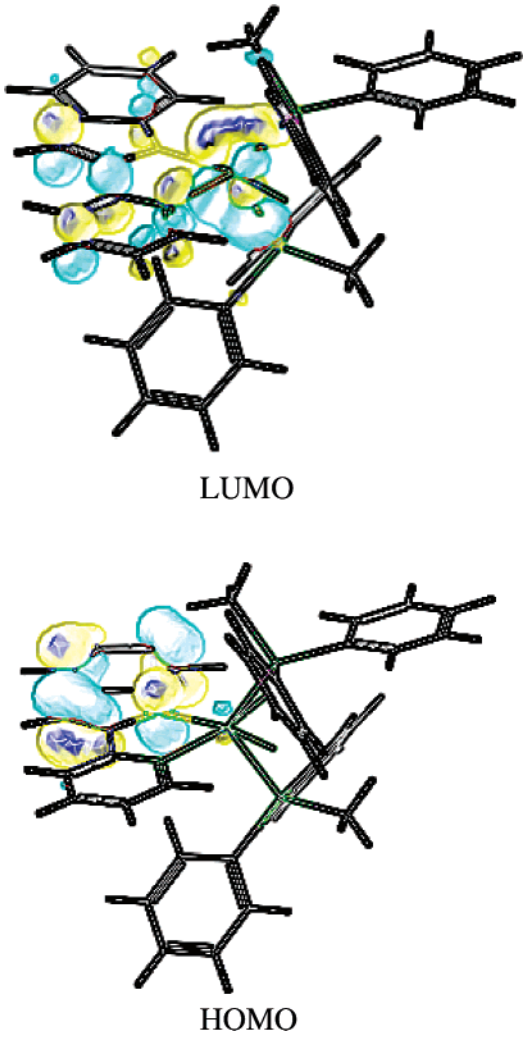

Figure 4. Jaguar representation of the frontier orbitals of **6c**, as determined by a DFT calculation.

Distortions from octahedral geometry in **6c** are expected on the basis of experimental[36] and theoretical[37] work on six-coordinate d^4 complexes. To probe the factors that cause this complex to adopt a bicapped tetrahedral structure, a DFT-B3LYP approach was used to calculate the frontier orbitals of **6c**. The atomic coordinates for **6c** were used as a starting point in the calculations, and an energy minimization was performed with the aid of the Jaguar software package (see Computational Details). The geometry of the energy-minimized structure does not deviate significantly from that of the solid-state structure of **6c**, as determined by X-ray crystallography. The calculated LUMO features a primarily metal-centered orbital that appears to be a hybrid between p_z and d orbitals (Figure 4) and has significant M−Si σ^* character. This hybrid orbital can also be derived by an analysis of orbital perturbations caused by a

(33) Jessop, P. G.; Morris, R. H. *Coord. Chem. Rev.* **1992**, *121*, 155.

(34) (a) Dioumaev, V. K.; Procopio, L. J.; Carroll, P. J.; Berry, D. H. *J. Am. Chem. Soc.* **2003**, *125*, 8043. (b) Dioumaev, V. K.; Yoo, B. R.; Procopio, L. J.; Carroll, P. J.; Berry, D. H. *J. Am. Chem. Soc.* **2003**, *125*, 8936.

(35) Reinartz, S.; White, P. S.; Brookhart, M.; Templeton, J. L. *J. Am. Chem. Soc.* **2001**, *123*, 6425.

(36) (a) Bernskoetter, W. H.; Lobkovsky, E.; Chirik, P. J. *Chem. Commun.* **2004**, 764. (b) Yang, S.-Y.; Leung, W.-H.; Lin, Z. *Organometallics* **2001**, *20*, 3198. (c) Kamato, M.; Hirotsu, K.; Higuchi, T.; Tatsumi, K.; Hoffman, R.; Yoshida, T.; Otsuka, S. *J. Am. Chem. Soc.* **1981**, *103*, 5772. (d) Templeton, J. L.; Ward, B. C. *J. Am. Chem. Soc.* **1980**, *102*, 6568. (e) Chisholm, M. H.; Huffman, J. C.; Kelly, R. L. *J. Am. Chem. Soc.* **1979**, *101*, 7615.

(37) Kubacek, P.; Hoffman, R. *J. Am. Chem. Soc.* **1981**, *103*, 4320.

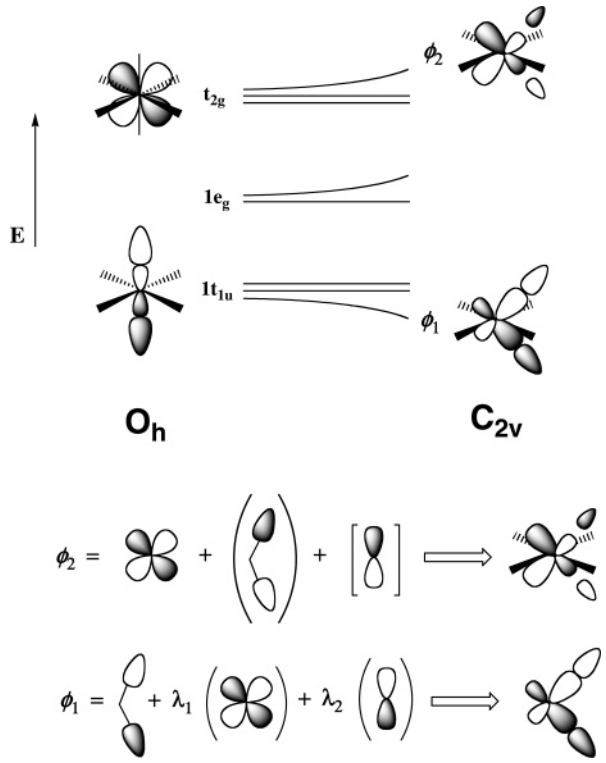

Figure 5. Molecular orbital analysis of the distortion from an octahedral to a bicapped tetrahedral geometry.

distortion from idealized octahedral geometry to a bicapped tetrahedral structure via bending of the two axial ligands toward one another.[38] One consequence of this deformation is an increase in energy for ϕ_2, a molecular orbital derived from the t_{2g} set (Figure 5). For a d^4 metal complex, this orbital becomes the LUMO, a result that accounts for the fact that the bicapped tetrahedral geometry is favored for this electron count. Additionally, the observed geometry and predicted molecular orbital structure of **6c** are consistent with the high *trans* influence of the silyl ligands and the presence of two strongly *trans*-influencing hydrides in the equatorial positions. Thus, if the two axial silyls are at 180° to one another, they must compete for the electron density in the same metal-based orbital (e.g., p_z and d_{z^2}). As these ligands bend away from the *z*-axis, however, the orbitals are rehybridized to lower the energies of the bonding Ir−Si interactions. This results in greatly increased stabilization of the bonding ϕ_1 orbital (Figure 5). Interestingly, the calculated HOMO of **6c** reflects a high degree of ligand-based character, suggesting that the distribution of negative charge on the anionic PyInd ligand dominates the electronic structure of this orbital (Figure 4).

(PyInd)Ir(III) Complexes. To further understand the effects of the d-electron count on the structures of (PyInd)Ir complexes, two Ir(III) derivatives were obtained. Reaction of **6a** with excess PMe_3 (5 equiv) at room temperature gave a single isomer of the d^6 complex (PyInd)IrH($SiEt_3$)(PMe_3)$_2$ (**7**) in 85% yield after the loss of 1 equiv of Et_3SiH (eq 6). The molecular structure of **7** exhibits a regular octahedral geometry (Figure 6), with the remaining silyl ligand occupying one of the axial positions. The hydride ligand, which adopts an equatorial rather than an axial position, was located in the Fourier difference map, and the Ir−H distance was determined to be 1.56(3) Å. The Ir−P bond length for the phosphine *trans* to the silyl group is 2.388(2),

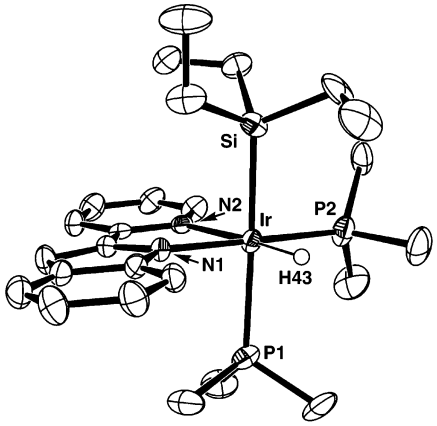

Figure 6. ORTEP diagram of the molecular structure of (PyInd)IrH($SiEt_3$)(PMe_3)$_2$ (**7**). Hydrogen atoms, except for the iridium hydride, were omitted for clarity. Selected bond lengths (Å): Ir−P1 = 2.388(2), Ir−P2 = 2.249(2), Ir−Si = 2.416(2), Ir−N1 = 2.079(4), Ir−N2 = 2.163(4), Ir−H43 = 1.56(3). Selected bond angles (deg): P1−Ir−P2 = 95.13(6), P1−Ir−Si = 168.49(5), P2−Ir−Si = 92.24(6), N1−Ir−N2 = 76.7(2), P1−Ir−H = 84(2), P2−Ir−H = 81(1), Si−Ir−H1 = 88(2).

significantly longer than that for the equatorial phosphine, Ir−P = 2.249(2) Å. Additionally, the fact that the hydride adopts the position *trans* to the pyridinyl, rather than the indolyl, can be rationalized by the expected, greater *trans* influence of the indolyl (vs the pyridinyl) group.[39]

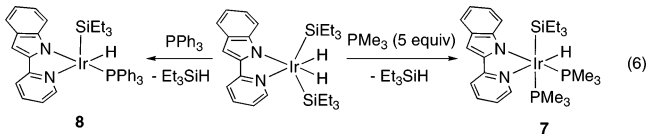

(6)

The ^{1}H NMR spectrum of **7** features a hydride resonance at −19.82 ppm, which exhibits coupling to the phosphorus atoms of the two PMe_3 ligands (J_{PH} = 22.5 Hz, $J_{P'H}$ = 10.5 Hz). A ^{29}Si{^{1}H-INEPT} spectrum of **7** features a resonance at 0.3 ppm (J_{SiP} = 151.3 Hz, J_{SiP} = 14.5 Hz) and is consistent with the positioning of the phosphines in the solid-state structure.[13a] The value of the coupling constant between the hydride and the ^{29}Si nucleus in this Ir(III) complex, determined by a *J*-resolved ^{1}H−^{29}Si gHMBC experiment, is 5.1 Hz, which is not significantly different form those for the hydrides in the Ir(V) complex **6a** (Table 2).

Complex **6a** also reacted with 1 equiv of PPh_3 at room temperature to give 1 equiv of Et_3SiH and an 80:20 mixture of isomers with the formulation (PyInd)IrH($SiEt_3$)(PPh_3), as judged by ^{1}H and ^{31}P{^{1}H} NMR spectroscopy. Upon heating in benzene at 80 °C for 2 h, this mixture was completely converted to the major isomer **8**, a monophosphine Ir(III) complex that was isolated in 91% yield (eq 6). Although the location of the hydride ligand in the X-ray crystal structure of **7** (Figure 7) was determined, the estimated standard deviation in the measurement of the Ir−H distance (1.51(8) Å) is quite large, preventing meaningful comparisons with Ir−H bond lengths in other complexes. As with **7**, the placement of the hydride *trans* to the pyridinyl is consistent with predictions based on the relative *trans* influence of the two nitrogen donors of PyInd.

The molecular geometry of **8** can be described as a distorted square pyramid, featuring four ligands that are all slightly below the basal plane of the molecule. In addition, the axial silyl group is bent away from the PyInd ligand, and the Ir−Si bond vector

(38) Albright, T. A.; Burdett, J. K.; Whangbo, M.-H. *Orbital Interactions in Chemistry*; Wiley: New York, 1985; pp 289−294.

(39) Lersch, M.; Tilset, M. *Chem. Rev.* **2005**, *105*, 2471.

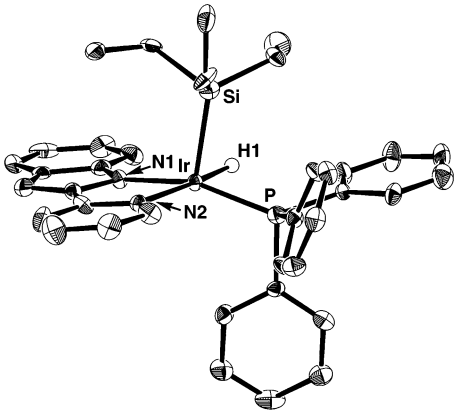

Figure 7. ORTEP diagram of the molecular structure of (PyInd)IrH($SiEt_3$)(PPh_3) (**8**). Hydrogen atoms were omitted for clarity. Selected bond lengths (Å): Ir−P = 2.234(2), Ir−Si = 2.315(2), Ir−N1 = 2.037(6), Ir−N2 = 2.168(6), Ir−H1 = 1.51(8). Selected bond angles (deg): P−Ir−Si = 97.83(7), P−Ir−H1 = 79(3), Si−Ir−H1 = 80(3), N1−Ir−H1 = 99(3), N2−Ir−H1 = 176(2), N1−Ir−N2 = 77.3(2).

forms an angle of approximately 74° with the basal plane. While the Si−Ir−P angle is approximately 97.8°, the Si−Ir−H1 angle is significantly smaller (80°), indicating that the silyl ligand "leans" toward the hydride. Nevertheless, the Si−H distance of approximately 2.5 Å is too long to invoke η^2-silane complex character in **8**.

The ^{1}H NMR spectrum of **8** exhibits a hydride resonance at −16.76 ppm (J_{PH} = 21.0 Hz). The ^{29}Si{^{1}H-INEPT} spectrum of **8**, which contains a resonance at 25.9 ppm (J_{SiP} = 8.8 Hz), confirms the *cis* positioning of the triethylsilyl ligand and PPh_3, as indicated by the low value of the Si−P coupling constant.[13a] Moreover, the value of the Si−H coupling constant, 6.0 Hz, is similar to those found for other hydrides described herein. In general, the successful synthesis of d^6 Ir(III) complexes **7** and **8**, which feature common octahedral and distorted square pyramidal geometries, respectively, reinforces the notion that the d^4 electron configuration is an important factor in determining the unusual structure of the Ir(V) bis(silyl)dihydride **6c**.

Conclusions

Rhodium and iridium complexes containing the PyInd ligand exhibit rich Si−H bond activation chemistry that leads to interesting catalytic and stoichiometric processes. A (PyInd)Rh(I) precursor catalyzes the dehydrochlorinative coupling of chlorobenzene with triethylsilane, which appears to involve an unusual Rh(V) bis(silyl)dihydride intermediate. The (PyInd)Ir fragment provides a platform for the isolation and characterization of several pentavalent bis(silyl)dihydrides that are analogous to the catalytically active rhodium species. Structural characterizations, DFT calculations, and reactivity studies establish that observed structural distortions are a likely consequence of the d^4 electron count and the presence of strongly *trans*-influencing silyl ligands in these complexes.

Studies by other researchers have pointed to the importance of M(V) (M = Ir, Rh) silyl or boryl intermediates in catalytic processes such as dehydrogenative coupling reactions of arenes with silanes or boranes, respectively.[6a,11a,40] The present report demonstrates that such intermediates also play a role in catalytic activations involving silanes and the C−Cl bond of chlorbenzene. In addition, utilization of the bidentate, monoanionic ligand PyInd, rather than more common L_2X-type ligands based on the cyclopentadielyl or tris(pyrazolyl)borate frameworks, leads to the formation of unusual six-coordinate 16-electron complexes.[41] Such species appear to mediate substrate activations by an unusual process, involving an associative step with a seven-coordinate intermediate or, alternatively, a dissociative process requiring reductive elimination from a 16-electron complex. The results described herein provide impetus for further synthetic and mechanistic studies of six-coordinate complexes of the type (NN*)MX_4 (M = Rh, Ir).

Experimental Section

Synthetic Methods. All experiments were conducted under a nitrogen atmosphere using standard Schlenk techniques or in a Vacuum Atmospheres drybox, unless otherwise noted. Dry, oxygen-free solvents were used throughout. Olefin impurities were removed from pentane by treatment with concentrated H_2SO_4, 0.5 N $KMnO_4$ in 3 M H_2SO_4, and saturated $NaHCO_3$. Pentane was then dried over $MgSO_4$, stored over activated 4 Å molecular sieves, and distilled over potassium benzophenone ketyl under a nitrogen atmosphere. Thiophene impurities were removed from benzene by treatment with H_2SO_4 and saturated $NaHCO_3$. Benzene was then dried over $MgSO_4$ and distilled from potassium metal under a nitrogen atmosphere. Chlorobenzene and dichloromethane were distilled from CaH_2.

Deuterated solvents were purchased from Cambridge Isotopes and dried with appropriate drying agents. Unless otherwise noted, all reagents were purchased from Aldrich or Gelest Chemicals and used without further purification. Liquid silanes were stored over activated molecular sieves, and 1-octene was dried over sodium metal and then vacuum-transferred onto activated molecular sieves before use. The compounds K[PyInd],[17a] $[(CO)_2RhCl]_2$,[42] $[(COD)RhCl]_2$,[43] $[(C_2H_4)_2RhCl]_2$,[44] and $[(COE)_2IrCl]_2$[45] were prepared according to literature procedures, while $[(COD)IrCl]_2$ was obtained from Strem Chemicals.

Analytical Methods. Routine NMR spectra were recorded at room temperature, using a Bruker DRX-500 spectrometer equipped with a 5 mm BBI probe or a Bruker AV-500 spectrometer equipped with a 5 mm BB probe. ^{1}H (500.1 MHz) and ^{13}C{^{1}H} (124.7 MHz) NMR spectra were referenced internally by the residual solvent signal relative to tetramethylsilane, while ^{29}Si{^{1}H} (99.7 MHz) NMR spectra were referenced to an external tetramethylsilane standard and ^{31}P{^{1}H} (202.5 MHz) NMR spectra were referenced to an external 85% H_3PO_4 standard. Unless otherwise noted, spectra for all NMR-active nuclei of a given compound were obtained in the same solvent. Multiplets that are predicted to be doublets of doublets but appear as pseudotriplets are denoted as "pt".

Elemental analyses were performed by the College of Chemistry Microanalytical Laboratory at the University of California, Berkeley. FT-infrared spectra were recorded as KBr pellets using a Mattson FTIR 3000 spectrometer at a resolution of 4 cm^{-1}. Identities of organic products were confirmed by ^{1}H NMR spectroscopy and by GC-MS, using an Agilent Technologies 6890N GC system with an HP-5MS column.

(PyInd)Rh(CO)$_2$ (1). To a stirred suspension of $[(CO)_2RhCl]_2$ (0.126 g, 0.323 mmol) in 5 mL of benzene was added K[PyInd] (0.150 g, 0.646 mmol) as a solid. The reaction mixture was stirred

(40) (a) Hartwig, J. F.; Cook, K. S.; Hapke, M.; Incarvito, C. D.; Fan, Y.; Webster, C. E.; Hall, M. B. *J. Am. Chem. Soc.* **2005**, *127*, 2538. (b) Webster, C. E.; Hall, M. B. *Coord. Chem. Rev.* **2003**, *238*, 315. (c) Kawamura, K.; Hartwig, J. F. *J. Am. Chem. Soc.* **2001**, *123*, 8422.

(41) For related work with β-diiminate ligands on Rh and Ir, see: Bernskoetter, W. H.; Lobkovsky, E.; Chirik, P. J. *Organometallics* **2005**, *24*, 4367, and refs 21 and 36a.

(42) McCleverty, J. A.; Wilkinson, G. *Inorg. Synth.* **1990**, *28*, 84.

(43) Giordano, G.; Crabtree, R. H. *Inorg. Synth.* **1990**, *28*, 88.

(44) Cramer, R. *Inorg. Synth.* **1990**, *28*, 86.

(45) van der Ent, A.; Onderdelinden, A. L. *Inorg. Synth.* **1990**, *28*, 90.

at room temperature for 16 h, and the solvent was removed in vacuo. The resulting solid was extracted with 10 mL of dichloromethane and filtered, the solvent volume was reduced to 2 mL, and the resulting solution was layered with 5 mL of pentane and stored at −35 °C for 2 days, yielding **1** as a dark green powder (0.173 g, 76%). ^{1}H NMR (dichloromethane-d_2): δ 6.95 (m, 4H), 7.12 (pt, ^3J = 7.2 Hz, 1H), 7.47 (d, ^3J = 8.5 Hz, 1H), 7.55 (d, ^3J = 7.5 Hz, 1H), 7.76 (s, 1H), 8.34 (d, ^3J = 5.0 Hz, 1H). ^{13}C{^{1}H} NMR: δ 103.2, 115.3, 119.0, 120.1, 121.0, 121.4, 123.4, 130.2, 139.2, 146.8, 147.2, 151.4, 157.9. IR (cm^{-1}): 1999 (s, ν_{CO}), 2054 (s, ν_{CO}). Anal. Calcd for $C_{15}H_9N_2O_2Rh$: C, 51.16; H, 2.58; N, 7.95. Found: C, 50.86; H, 2.45; N, 8.26.

(PyInd)Rh(COD) (2). To a stirred suspension of [(COD)RhCl]$_2$ (0.212 g, 0.430 mmol) in 6 mL of benzene was added K[PyInd] (0.200 g, 0.861 mmol) as a solid. The reaction mixture was stirred at room temperature for 16 h, and the solvent was removed in vacuo. The resulting solid was extracted with 8 mL of dichloromethane and filtered, the solvent volume was reduced to 3 mL, and the resulting solution was layered with 10 mL of pentane and stored at −35 °C for 2 days, yielding **2** as a yellow crystalline solid (0.324 g, 93%). ^{1}H NMR (dichloromethane-d_2): δ 1.99 (m, 2H, CH_2), 2.09 (m, 2H, CH_2), 2.54 (m, 4H, CH_2), 4.05 (d, ^3J = 2.0 Hz, 2H, C*H*), 5.47 (d, ^3J = 2.5 Hz, 2H, C*H*), 6.87 (pt, ^3J = 6.8 Hz, 1H), 6.89 (s, 1H), 6.95 (m, 2H), 7.00 (pt, ^3J = 7.0 Hz, 1H), 7.50 (pt, ^3J = 6.8 Hz, 2H), 7.67 (d, ^3J = 7.5 Hz, 1H), 7.73 (d, ^3J = 8.0 Hz, 1H). ^{13}C{^{1}H} NMR: δ 30.0, 31.5, 78.8 (d, J_{RhC} = 12.5 Hz), 79.4 (d, J_{RhC} = 11.3 Hz), 101.8, 114.3, 118.0, 119.9, 120.7, 120.9, 122.1, 131.5, 138.2, 145.6, 147.1, 147.7, 158.7. Anal. Calcd for $C_{21}H_{21}N_2Rh$: C, 62.38; H, 5.23; N, 6.61. Found: C, 61.99; H, 5.33; N, 6.61.

(PyInd)Rh(C$_2$H$_4$)$_2$ (3). To a stirred suspension of [(C$_2$H$_4$)$_2$RhCl]$_2$ (0.251 g, 0.645 mmol) in 5 mL of benzene was added K[PyInd] (0.300 g, 1.291 mmol) as a solid. The reaction mixture was stirred at room temperature for 16 h, and the solvent was removed in vacuo. The resulting solid was extracted with 15 mL of dichloromethane and filtered, the solvent volume was reduced to 5 mL, and 20 mL of pentane was added to the resulting solution, yielding a **3** as a red-orange powder (0.368 g, 81%). ^{1}H NMR (dichloromethane-d_2): δ 1.98 (br, 2H, C*H*), 2.39 (br, 2H, C*H*), 2.75 (br, 2H, C*H*), 4.82 (br, 2H, C*H*), 5.97 (pt, ^3J = 6.0 Hz, 1H), 6.61 (pt, ^3J = 7.0 Hz, 1H), 6.69 (d, ^3J = 6.0 Hz, 1H), 6.79 (s, 1H), 7.00 (d, ^3J = 8.0 Hz, 1H), 7.14 (m, 2H), 7.35 (d, ^3J = 8.5 Hz, 1H), 7.78 (d, ^3J = 7.5 Hz, 1H). ^{13}C{^{1}H} NMR: δ 60.8 (d, J_{RhC} = 12.5 Hz), 62.6 (br), 103.2, 114.3, 118.8, 119.4, 119.6, 121.6, 123.3, 132.2, 137.3, 142.2, 147.1, 147.8, 159.2. Anal. Calcd for $C_{17}H_{17}N_2Rh$: C, 57.97; H, 4.86; N, 7.95. Found: C, 57.68; H, 4.72; N, 7.73.

(PyInd)RhH$_2$(SiEt$_3$)$_2$ (4). To a stirred solution of **3** in benzene (0.080 g, 0.227 mmol) was added 4 equiv of Et$_3$SiH (0.106 g, 145 μL, 0.908 mmol) via syringe. The reaction mixture was stirred for 2 h at 60 °C in a Teflon-sealed flask and allowed to cool to room temperature, and volatile materials were then removed under reduced pressure. The resulting red oil was then lyophilized with benzene, rapidly washed with 3 mL of cold pentane, and dried in vacuo, yielding **4** as an oily, red solid (0.085 g, 71%). ^{1}H NMR (benzene-d_6): δ −15.32 ppm (dd, J_{RhH} = 28.5 Hz, ^2J = 9.0 Hz, 1H, Rh*H*), −13.88 ppm (J_{RhH} = 23.5 Hz, ^2J = 9.0 Hz, 1H, Rh*H*), 0.92−1.03 (two overlapping m, 30H, CH_2 and CH_3), 6.18 (pt, ^3J = 6.0 Hz, 1H), 6.75 (vt, ^3J = 7.3 Hz, 1H), 6.91 (s, 1H), 7.12 (m, obscured by solvent signal, 1H), 7.19 (pt, ^3J = 7.0 Hz, 1H), 7.41 (pt, ^3J = 8.0 Hz, 1H), 7.79 (d, ^3J = 8.0 Hz, 1H), 7.96 (d, ^3J = 8.0 Hz, 1H), 8.22 (pt, ^3J = 5.0 Hz, 1H). ^{13}C{^{1}H} NMR: δ 8.7, 12.7, 103.9, 118.3, 120.0, 120.3, 120.7, 121.6, 123.9, 132.1, 138.3, 148.1, 148.2, 152.3, 158.5. ^{29}Si{^{1}H} NMR: δ 63.0 (J_{RhSi} = 26.8 Hz). ^{29}Si NMR (via ^{1}H−^{29}Si gHMBC): δ 63.0 (J_{SiH} = 8.1 Hz, $J_{SiH'}$ = 6.2 Hz). IR (cm^{-1}): 2065 (br, ν_{RhH}), 2090 (br, ν_{RhH}). Anal. Calcd for $C_{25}H_{41}N_2Si_2Rh$: C, 56.80; H, 7.82; N, 5.30. Found: C, 56.75; H, 7.65; N, 5.18.

(PyInd)Ir(COD) (5). To a stirred suspension of [(COD)IrCl]$_2$ (0.289 g, 0.430 mmol) in 8 mL of benzene was added K[PyInd] (0.200 g, 0.861 mmol) as a solid. The reaction mixture was stirred at room temperature for 16 h, and the solvent was removed in vacuo. The resulting solid was extracted with 10 mL of dichloromethane and filtered, the solvent volume was reduced to 3 mL, and the resulting solution was layered with 10 mL of pentane and stored at −35 °C for 2 days, yielding **5** as a red microcrystalline solid (0.391 g, 92%). ^{1}H NMR (dichloromethane-d_2): δ 1.74 (m, 2H, CH_2), 1.92 (m, 2H, CH_2), 2.36 (m, 4H, CH_2), 3.66 (d, ^3J = 2.5 Hz, 2H, C*H*), 5.23 (d, ^3J = 3.0 Hz, 2H, C*H*), 6.92 (m, 2H), 7.03 (m, 3H), 7.53 (d, ^3J = 8.0 Hz, 1H), 7.77 (m, 3H). ^{13}C{^{1}H} NMR: δ 30.4, 32.6, 61.6, 64.3, 103.6, 114.6, 118.8, 119.8, 121.2 (two overlapping signals), 123.1, 132.3, 138.9, 145.7, 147.5, 149.8, 159.7. Anal. Calcd for $C_{21}H_{21}N_2Ir$: C, 51.10; H, 4.29; N, 5.67. Found: C, 50.79; H, 4.36; N, 5.58.

(PyInd)IrH$_2$(SiEt$_3$)$_2$ (6a). To the solids K[PyInd] (0.040 g, 0.172 mmol) and [(COE)$_2$IrCl]$_2$ (0.077 g, 0.086 mmol), which were placed in a vial, was added a solution of Et$_3$SiH (0.040 g, 55.0 μL, 0.344 mmol) in 5 mL of benzene with rapid stirring. The reaction mixture was stirred for 30 min and was filtered, and the solvent was then removed in vacuo. The remaining yellow oil was lyophilized from benzene, rapidly washed with 2 mL of cold pentane, and dried in vacuo, resulting in the formation of **6a** as an oily, yellow solid (0.070 g, 67%). ^{1}H NMR (benzene-d_6): δ −18.04 ppm (d, ^2J = 2.0 Hz, 1H, Ir*H*), −15.53 ppm (d, ^2J = 2.0 Hz, 1H, Ir*H*), 0.95 (s, 30H, overlapping CH_2 and CH_3), 6.09 (pt, ^3J = 6.4 Hz, 1H), 6.72 (pt, ^3J = 7.2 Hz, 1H), 6.78 (s, 1H), 7.03 (d, ^3J = 8.0 Hz, 1H), 7.12 (m, partially obscured by solvent signal, 1H), 7.37 (pt, ^3J = 7.6 Hz, 1H), 7.68 (d, ^3J = 8.0 Hz, 1H), 7.99 (d, ^3J = 8.4 Hz, 1H), 8.40 (d, ^3J = 5.6 Hz, 1H). ^{13}C{^{1}H} NMR: δ 8.7, 12.6, 118.9, 119.6, 121.3, 121.5, 121.7, 124.6, 132.3, 138.2, 149.0, 151.2, 154.0, 158.2, 159.5. ^{29}Si NMR (via ^{1}H−^{29}Si gHMBC): δ 37.1 (J_{SiH} = 6.4 Hz, $J_{SiH'}$ = 6.7 Hz). IR (cm^{-1}): 2094 (br, ν_{IrH}), 2162 (br, ν_{IrH}). Anal. Calcd for $C_{25}H_{41}N_2Si_2Ir$: C, 48.58; H, 6.69; N, 4.53. Found: C, 48.20; H, 6.73; N, 4.47.

(PyInd)IrH$_2$(SiMe$_2$Ph)$_2$ (6b). To the solids K[PyInd] (0.020 g, 0.086 mmol) and [(COE)$_2$IrCl]$_2$ (0.039 g, 0.043 mmol), which were placed in a vial, was added a solution of Me$_2$PhSiH (0.023 g, 26.4 μL, 0.172 mmol) in 3 mL of benzene with rapid stirring. The reaction mixture was stirred for 30 min and was filtered, and the solvent was then removed in vacuo. The remaining red oil was then lyophilized from benzene, rapidly washed with 1 mL of cold pentane, and dried in vacuo, resulting in the formation of **6b** as an oily, orange solid (0.042 g, 75%). ^{1}H NMR (benzene-d_6): δ −17.36 ppm (d, ^2J = 2.4 Hz, 1H, Ir*H*), −14.84 ppm (d, ^2J = 2.4 Hz, 1H, Ir*H*), 0.77 (s, 6H, CH_3), 0.80 (s, 6H, CH_3), 5.80 (pt, ^3J = 7.2 Hz, 1H), 6.58 (pt, ^3J = 7.6 Hz, 1H), 6.60 (s, 1H), 6.58 (d, ^3J = 7.5 Hz, 1H), 6.97 (m, 6H, *Ph*), 7.17 (pt, ^3J = 7.5 Hz, 1H), 7.37 (pt, ^3J = 8.0 Hz, 1H), 7.41 (m, 4H, *Ph*), 7.54 (d, ^3J = 5.5 Hz, 1H), 7.65 (pt, ^3J = 8.0 Hz, 1H), 7.85 (d, ^3J = 8.0 Hz, 1H). ^{13}C{^{1}H} NMR: δ 6.8, 7.3, 105.5, 118.9, 119.0, 121.1, 121.2, 121.4, 124.4, 127.6, 128.9, 132.4, 133.2, 137.6, 143.8, 148.6, 150.7, 153.9, 157.6. ^{29}Si NMR (via ^{1}H−^{29}Si gHMBC): δ 9.6 (J_{SiH} = 9.5 Hz, $J_{SiH'}$ = 12.1 Hz). IR (cm^{-1}): 2132 (br, ν_{IrH}), 2173 (br, ν_{IrH}). Anal. Calcd for $C_{29}H_{31}N_2Si_2Ir$: C, 53.10; H, 4.76; N, 4.27. Found: C, 53.33; H, 5.09; N, 4.48.

(PyInd)IrH$_2$(SiPh$_2$Me)$_2$ (6c). To the solids K[PyInd] (0.020 g, 0.086 mmol) and [(COE)$_2$IrCl]$_2$ (0.036 g, 0.043 mmol), which were placed in a vial, was added a solution of Ph$_2$MeSiH (0.034 g, 34.3 μL, 0.172 mmol) in 3 mL of benzene with rapid stirring. The reaction mixture was stirred for 30 min and was filtered, and the volume of the resulting solution was reduced to ca. 1 mL. This solution was diluted with 5 mL of pentane and stored at −35 °C for 2 days, leading to the precipitation of **6c** as a microcrystalline, red-orange solid (0.055 g, 82%). ^{1}H NMR (benzene-d_6): δ −16.59 ppm (d, ^2J = 2.5 Hz, 1H, Ir*H*), −13.87 ppm (d, ^2J = 2.5 Hz, 1H,

Ir*H*), 0.96 (s, 6H, CH_3), 5.73 (pt, ^3J = 7.2 Hz, 1H), 6.64 (pt, ^3J = 7.5 Hz, 1H), 6.73 (s, 1H), 6.81 (d, ^3J = 8.0 Hz, 1H), 6.91 (m, 6H, *Ph*), 7.10 (m, 6H, *Ph*), 7.18 (m, obscured by solvent signal, 1H), 7.26 (pt, ^3J = 7.5 Hz, 1H), 7.58 (m, 10H, *Ph* + obscured ligand resonances), 7.77 (d, ^3J = 8.0 Hz, 1H). ^{13}C{^{1}H} NMR: δ 6.7, 103.9, 116.5, 119.1, 119.2, 121.3, 121.4, 121.6, 124.6, 130.4, 130.7, 132.3, 135.0 (two overlapping signals), 135.1 (two overlapping signals), 140.9, 142.1, 148.2, 151.2, 153.8, 157.2. ^{29}Si NMR (via ^{1}H−^{29}Si gHMBC): δ 7.2 (J_{SiH} = 11.7 Hz, $J_{SiH'}$ = 14.2 Hz). IR (cm^{-1}): 2164 (br, ν_{IrH}), 2201 (br, ν_{IrH}). Anal. Calcd for $C_{39}H_{37}N_2Si_2Ir$: C, 59.89; H, 4.77; N, 3.58. Found: C, 60.28; H, 4.88; N, 3.59.

(PyInd)IrH$_2$(SiPh$_3$)$_2$ (6d). To the solids K[PyInd] (0.020 g, 0.086 mmol) and [(COE)$_2$IrCl]$_2$ (0.036 g, 0.043 mmol), which were placed in a vial, was added a solution of Ph_3SiH (0.045 g, 0.172 mmol) in 3 mL of benzene with rapid stirring. The reaction mixture was stirred for 30 min and was filtered, and the volume of the resulting solution was reduced to ca. 1 mL. This solution was layered with 5 mL of pentane and stored at room temperature for 2 days, leading to the precipitation of **6d** as a microcrystalline, red-orange solid (0.062 g, 79%). ^{1}H NMR (benzene-d_6): δ −16.06 ppm (d, ^2J = 2.8 Hz, 1H, Ir*H*), −13.05 ppm (d, ^2J = 2.8 Hz, 1H, Ir*H*), 5.72 (pt, ^3J = 7.2 Hz, 1H), 6.52 (pt, ^3J = 5.6 Hz, 1H), 6.55 (s, 1H), 6.80 (d, ^3J = 8.0 Hz, 1H), 6.98 (m, 18H, *Ph*), 7.05 (pt, ^3J = 6.8 Hz, 1H), 7.55 (pt, ^3J = 8.6 Hz, 1H), 7.75 (m, 13H, *Ph* + obscured ligand resonance), 7.78 (d, ^3J = 7.0 Hz, 1H), 7.83 (pt, ^3J = 7.2 Hz, 1H). ^{13}C{^{1}H} NMR: δ 104.5, 127.2, 128.4, 128.6, 129.3, 130.1, 133.8, 136.1 (two overlapping signals), 136.2 (two overlapping signals), 139.3, 140.0, 142.2, 143.1, 148.2, 153.5, 158.9. ^{29}Si NMR (via ^{1}H−^{29}Si gHMBC): δ 9.2 (J_{SiH} = 12.5 Hz, $J_{SiH'}$ = 17.4 Hz). IR (cm^{-1}): 2170 (br, ν_{IrH}), 2194 (br, ν_{IrH}). Anal. Calcd for $C_{49}H_{41}N_2Si_2Ir$: C, 64.73; H, 4.55; N, 3.08. Found: C, 64.71; H, 4.45; N, 3.38.

(PyInd)IrH(SiEt$_3$)(PMe$_3$)$_2$ (7). To a stirred solution of **6a** (0.025 g, 0.040 mmol) in 2 mL of benzene was added 5 equiv of PMe_3 (0.015 g, 21.0 μL, 0.202 mmol) via syringe. The reaction mixture was stirred for 30 min. The reaction volume was then reduced to ca. 1 mL, and the resulting solution was layered with 5 mL of pentane and stored for 2 days at room temperature, leading to the precipitation of **7** as a bright yellow powder (0.026 g, 85%). ^{1}H NMR (benzene-d_6): δ (dd, −19.82 ppm, J_{PH} = 22.5 Hz, $J_{P'H}$ = 10.5 Hz, 1H, Ir*H*), 0.33 (d, J_{PH} = 7.0 Hz, 9H, P*Me*$_3$), 0.39 (m, 3H, CH_2), 0.65 (m, 3H, CH_2), 0.90 (pt, ^3J = 8.0 Hz, 9H, CH_3), 1.32 (d, J_{PH} = 8.5 Hz, 9H, P*Me*$_3$), 6.24 (pt, ^3J = 6.0 Hz, 1H), 6.93 (pt, ^3J = 7.5 Hz, 1H), 7.17 (pt, ^3J = 7.5 Hz, 1H), 7.20 (s, 1H), 7.34 (pt, ^3J = 7.5 Hz, 1H), 7.42 (d, ^3J = 8.0 Hz, 1H), 7.74 (d, ^3J = 8.5 Hz, 1H), 7.89 (d, ^3J = 8.0 Hz, 1H), 8.26 (d, ^3J = 6.5 Hz, 1H). ^{13}C{^{1}H} NMR: δ 8.1 (d, $^3J_{PC}$ = 6.3 Hz), 9.3, 16.7 (d, $^1J_{PC}$ = 17.5 Hz), 22.0 (dd, $^1J_{PC}$ = 36.3 Hz, $^3J_{P'C}$ = 5.0 Hz), 101.5, 118.7, 119.2, 119.6, 119.8, 121.7, 122.1, 130.8, 135.2, 145.7, 146.4, 151.4, 159.5. ^{29}Si NMR (via ^{1}H−^{29}Si gHMBC): 0.3 ppm (J_{SiH} = 5.1 Hz). ^{29}Si{^{1}H-INEPT}: δ 0.3 ppm (dd, J_{SiP} = 151.3 Hz, $J_{SiP'}$ = 14.5 Hz). ^{31}P{^{1}H} NMR: δ −52.2 ppm (d, J_{PP} = 11.3 Hz), −41.7 ppm (d, J_{PP} = 11.3 Hz). IR (cm^{-1}): 2153 (s, ν_{IrH}). Anal. Calcd for $C_{25}H_{42}N_2P_2SiIr$: C, 45.99; H, 6.48; N, 4.29. Found: C, 45.95; H, 6.61; N, 4.13.

(PyInd)IrH(SiEt$_3$)(PPh$_3$) (8). To a stirred solution of **6a** (0.025 g, 0.040 mmol) in 2 mL of benzene was added PPh_3 (0.011 g, 0.040 mmol) as a solid. The reaction mixture was stirred for 2 h at 80 °C in a Teflon-sealed flask and allowed to cool to room temperature, and the reaction volume was then reduced to ca. 1 mL. The resulting solution was layered with 5 mL of pentane and stored for 2 days at room temperature, leading to the precipitation of **8** as a yellow-orange, microcrystalline solid (0.028 g, 91%). ^{1}H NMR (benzene-d_6): δ −16.76 ppm (d, J_{PH} = 21.0 Hz, 1H, Ir*H*), 0.65−0.73 (two overlapping m, 12H, CH_3 + CH_2), 0.80 (m, 3H, CH_2), 6.13 (pt, ^3J = 6.0 Hz, 1H), 6.92 (pt, ^3J = 7.0 Hz, 1H), 7.10 (m, 6H, P*Ph*$_3$), 7.20 (s, 1H), 7.35 (d, ^3J = 7.0 Hz, 1H), 7.42 (d, ^3J = 8.0 Hz, 1H), 7.55 (pt, ^3J = 7.0 Hz, 1H), 7.81 (m, 9H, P*Ph*$_3$), 7.96 (d, ^3J = 8.0 Hz, 1H), 8.02 (d, ^3J = 5.0 Hz, 1H), 8.44 (d, ^3J = 8.0 Hz, 1H). ^{13}C{^{1}H} NMR: δ 8.7, 10.5, 104.8, 119.7, 119.8, 120.3, 120.6, 121.8, 123.5, 128.8, 130.4, 132.3, 134.3, 134.4, 134.8, 135.2, 137.4, 149.5, 151.2. ^{29}Si NMR (via ^{1}H−^{29}Si gHMBC): 25.9 ppm (J_{SiH} = 6.0 Hz). ^{29}Si{^{1}H-INEPT}: δ 25.9 ppm (d, J_{SiP} = 8.8 Hz). ^{31}P{^{1}H} NMR: δ 19.3 ppm. IR (cm^{-1}): 2199 (s, ν_{IrH}). Anal. Calcd for $C_{37}H_{40}N_2PSiIr$: C, 58.17; H, 5.28; N, 3.67. Found: C, 57.82; H, 5.15; N, 3.43.

General Procedure for Catalytic Runs. Reactions were conducted in 5 mm Wilmad NMR tubes equipped with a J. Young Teflon-valve seal, which were heated in temperature-controlled oil baths. Samples were prepared in a drybox by dissolving the catalyst and the specified reagents in neat chlorobenzene. Reaction progress was monitored by ^{1}H NMR spectroscopy (a small amount of cyclohexane-d_{12} was added to all samples in order to obtain a lock signal). Product yields were quantified by GC, using a calculated response factor to account for the difference in ionization between the integration standard (tetraphenylsilane) and phenyltriethylsilane.

Reaction of 4 with 1-Octene. To a sample of **4** (0.010 g, 0.019 mmol) dissolved in 0.5 mL of benzene-d_6 was added 5 equiv of 1-octene (0.014 g, 15 μL, 0.095 mmol) via microsyringe in a drybox. The resulting mixture was transferred to an NMR tube equipped with a Teflon-valve seal and heated to 70 °C. ^{1}H NMR spectra of this reaction mixture were obtained every 30 min, indicating complete consumption of 1-octene after 4 h. Analysis of organic reaction products by GC-MS indicated complete conversion of the starting 1-octene to a mixture of internal 1-octenes.

Reaction of 4 with PMe$_3$. To a sample of **4** (0.010 g, 0.019 mmol) dissolved in 0.5 mL of benzene-d_6 was added 10 equiv of PMe_3 (0.0048 g, 20 μL, 0.190 mmol) via microsyringe in a drybox. The resulting reaction mixture was analyzed by NMR spectroscopy, indicating liberation of 2 equiv of Et_3SiH (by ^{1}H NMR) and the formation of a Rh-containing species with the following spectroscopic properties. ^{1}H NMR: δ 0.77 (br, P*Me*$_3$, partially obscured by free PMe_3 signal), 1.14 (d, J_{PH} = 6.4 Hz, 9H, P*Me*$_3$), 6.78 (pt, ^3J = 6.0 Hz, 1H), 7.4 (m, 3H), 8.12 (d, ^3J = 8.0 Hz, 1H), 8.18 (s, 1H), 8.41 (d, ^3J = 7.6 Hz, 1H), 8.73 (d, ^3J = 4.8 Hz, 1H), 9.88 (d, ^3J = 8.0 Hz, 1H). ^{31}P{^{1}H} NMR: δ −11.4 ppm (br d, J_{RhP} = 139 Hz), −5.6 ppm (br d, J_{RhP} = 157 Hz). The presence of a new set of ligand resonances in the ^{1}H NMR spectrum and the appearance of two inequivalent Rh-coupled doublets in the ^{31}P{^{1}H} NMR spectrum, along with the observation of 2 equiv of free Et_3SiH, led to the assignment of the product as (PyInd)Rh(PMe$_3$)$_2$. Removal of solvent from this reaction mixture resulted in the formation of intractable materials.

General Considerations for X-ray Structure Determinations. The X-ray analyses of compounds **2**, **6c**, **7**, and **8** were carried out at the UC Berkeley CHEXRAY crystallographic facility. Measurements were made on a Bruker SMART CCD area detector with graphite-monochromated Mo Kα radiation (λ = 0.71069 Å). Data were integrated by the program SAINT and analyzed for agreement using XPREP. Empirical absorption corrections were made using SADABS. Structures were solved by direct methods and expanded using Fourier techniques. All calculations were performed using the teXsan crystallographic software package. Selected crystal and structure refinement data are summarized in Table 3.

X-ray Structure Determination of 2. X-ray-quality crystals of **2** formed upon vapor diffusion of diethyl ether into a dichloromethane solution at room temperature. There are two crystallographically independent molecules of the complex in the asymmetric unit of the primitive monoclinic space group $P2_1/n$. The primary difference between the two molecules is the slight rotation of the pyridine ring with respect to the indole fragment in one molecule (dihedral angle of 11°), while in the other molecule the two ligand fragments are nearly coplanar (dihedral angle of 1°).

Table 3. Summary of Crystallographic Data for Compounds 2, 6c, 7, and 8

	2	**6c**
formula	$RhN_2C_{21}H_{22}$	$IrSi_2N_2C_{39}H_{22}$
MW	405.32	782.13
cryst color, habit	orange, tablet	orange, block
cryst dimens	0.21 × 0.21 × 0.06 mm	0.16 × 0.16 × 0.05 mm
cryst syst	monoclinic	triclinic
lattice type	primitive	primitive
cell determination (2θ range)	3425 ($5.09° < 2\theta < 48.88°$)	5225 ($7.00° < 2\theta < 52.00°$)
lattice params	$a = 12.3332(9)$ Å	$a = 10.7460(7)$ Å
	$b = 10.7187(8)$ Å	$b = 11.5942(8)$ Å
	$c = 24.159(2)$ Å	$c = 14.648(1)$ Å
		$\alpha = 98.463(1)°$
	$\beta = 93.987(1)°$	$\beta = 98.369(1)°$
		$\gamma = 110.232(1)°$
	$V = 3186(4)$ Å^3	$V = 1655.3(2)$ Å^3
space group	$P2_1/n$ (#14)	$P\bar{1}$ (#2)
Z value	8	2
D_{calc}	1.690 g/cm^3	1.569 g/cm^3
μ(Mo Kα)	10.73 cm^{-1}	41.47 cm^{-1}
temperature	−154 °C	−112 °C
scan type	ω (0.3° per frame)	ω (0.3° per frame)
no. of reflns measd	total: 13 668	total: 13 575
	unique: 5592 ($R_{int} = 0.062$)	unique: 6818 ($R_{int} = 0.020$)
corrections	Lorentz−polarization	Lorentz−polarization
	abs ($T_{max} = 1.00$, $T_{min} = 0.61$)	abs ($T_{max} = 1.00$, $T_{min} = 0.82$)
structure solution	direct methods (SIR97)	direct methods (SIR97)
refinement	full-matrix least squares	full-matrix least squares
no. reflns obsd	3336 [$I > 3.0\sigma(I)$]	5811 [$I > 3.0\sigma(I)$]
no. variables	433	403
R; R_w; R_{all}	0.037; 0.039; 0.072	0.023; 0.027; 0.028
GOF	1.27	1.16
max. peak in final diff map	1.02 e$^-$/Å^3	1.18 e$^-$/Å^3
min. peak in final diff map	−0.94 e$^-$/Å^3	−0.47 e$^-$/Å^3

	7	**8**
formula	$IrP_2SiN_2C_{25}H_{42}$	$IrPSi_2N_2C_{37}H_{40}$
MW	652.87	764.02
cryst color, habit	yellow, blade	red, blocklike
cryst dimens	0.20 × 0.08 × 0.01 mm	0.04 × 0.10 × 0.17 mm
cryst syst	monoclinic	orthorhombic
lattice type	primitive	primitive
cell determination (2θ range)	2185 ($5.00° < 2\theta < 44.00°$)	5295 ($5.00° < 2\theta < 49.00°$)
lattice params	$a = 12.183(1)$ Å	$a = 10.979(1)$ Å
	$b = 14.839(2)$ Å	$b = 15.360(1)$ Å
	$c = 15.701(2)$ Å	$c = 19.484(2)$ Å
	$\beta = 91.057(2)°$	
	$V = 2838.0(6)$ Å^3	$V = 3285.7(5)$ Å^3
space group	$P2_1/n$ (#14)	$P2_12_12_1$ (#19)
Z value	4	4
D_{calc}	1.528 g/cm^3	1.544 g/cm^3
μ(Mo Kα)	48.87 cm^{-1}	41.88 cm^{-1}
temperature	−120 °C	−130 °C
scan type	ω (0.3° per frame)	ω (0.3° per frame)
no. of reflns measd	total: 15 929	total: 14 603
	unique: 6079 ($R_{int} = 0.048$)	unique: 3408 ($R_{int} = 0.073$)
corrections	Lorentz−polarization	Lorentz−polarization
	abs ($T_{max} = 1.00$, $T_{min} = 0.74$)	abs ($T_{max} = 1.00$, $T_{min} = 0.60$)
structure solution	direct methods (SIR97)	direct methods (SIR97)
refinement	full-matrix least squares	full-matrix least squares
no. reflns obsd	3830 [$I > 3.0\sigma(I)$]	4655 [$I > 3.0\sigma(I)$]
no. variables	283	364
R; R_w; R_{all}	0.032; 0.035; 0.062	0.034; 0.037; 0.046
GOF	1.11	1.16
max. peak in final diff map	1.43 e$^-$/Å^3	1.35 e$^-$/Å^3
min. peak in final diff map	−0.66 e$^-$/Å^3	−1.50 e$^-$/Å^3

X-ray Structure Determination of 6c. This complex crystallizes upon vapor diffusion of pentane into a toluene solution at room temperature. There are two molecules of **6c** in the unit cell of the primitive, triclinic space group $P\bar{1}$. The positions of the hydrides were observed in the Fourier difference map and were included with a restrained distance of 1.65 Å to Ir.

X-ray Structure Determination of 7. The complex crystallizes upon vapor diffusion of pentane into a benzene solution at room temperature. There are four molecules of **7** in the unit cell of the primitive monoclinic space group $P2_1/n$. The iridium center exhibits a slightly distorted octahedral coordination geometry. The hydride was located in a difference Fourier map and was included in a refined position (Ir−H distance = 1.53 Å).

X-ray Structure Determination of 8. X-ray quality crystals of complex **8** were obtained by slow evaporation of a dilute benzene solution. The compound crystallizes in the chiral space group

$P2_12_12_1$ with one molecule in the asymmetric unit. The enantiomorph of the space group and enantiomer of the molecule were determined by inspection of Friedel pairs of reflections followed by comparison of least-squares refinements. The results were unequivocal in favor of the enantiomorph reported. The hydride was located in a Fourier difference map, and its positional parameters were refined with a fixed thermal parameter.

Computational Details

Method. Quantum mechanical calculations were performed at the University of California, Berkeley, Molecular Graphics Facility using a 98 cpu-cluster with 2.8 GHz Xeon processors. The DFT calculation on **6c** was carried out by implementing the B3LYP exchange−correlation functional[46] with the LACVP**++ basis set using Jaguar 5.5. The geometry of **6c** was fully optimized in the gas phase without symmetry constraints. Vibrational frequencies were calculated to ensure that local minima lacked any negative frequencies.

(46) (a) Becke, A. D. *J. Chem. Phys.* **1993**, *98*, 5648. (b) Lee, C.; Yang, W.; Parr, R. G. *Phys. Rev. B* **1988**, *37*, 785.

Acknowledgment is made to Dr. Herman van Halbeek for assistance with the ^{29}Si NMR experiments, to Dr. Fred Hollander and Dr. Allen Oliver for assistance with the X-ray crystallography, and to Dr. Kathy Durkin for training at the Molecular Graphics Facility. This work was supported by the Director, Office of Energy Research, Office of Basic Energy Sciences, Chemical Sciences Division, of the U.S. Department of Energy under Contract No. DE-AC02-05CH11231.

Supporting Information Available: X-ray crystallographic data for **2**, **6c**, **7**, and **8** (CIF). This material is available free of charge via the Internet at http://pubs.acs.org.

OM060492+